K-5

LOW-LOSS 360° X-BAND ANALOG PHASE SHIFTER

John I. Upshur and Bernard D. Geller

COMSAT Laboratories
Clarksburg, Maryland 20871

Abstract

A low-loss reflection-type analog phase shifter circuit is described and experimental results are presented. The circuit incorporates several design features to produce nearly 360° of phase shift at X-band while achieving an insertion loss of only 4.8 dB with ±0.5 dB of variation over all phase states. These results improve upon previously reported X-band performance by demonstrating a large phase shift range together with low attenuation and low amplitude variation with phase state.

INTRODUCTION

The MIC analog phase shifter described here is part of a larger task, the goal of which is the development of a fully monolithic GaAs unit. These circuits are intended for applications to phased array antennas, where insertion loss should be small and, ideally, constant over all phase states to achieve high system performance without the need for additional compensating circuitry. Unlike digital phase shifter approaches, the available phase resolution of the analog phase shifter depends primarily on the number of bits in the D/A converter. Therefore, higher levels of resolution do not result in significant increases in circuit complexity or insertion loss. The analog phase shifter may also be made smaller than the digital phase shifter resulting in higher circuit yield and lower cost.

Previously reported phase shifter results at X-band have not simultaneously demonstrated a full 360° phase shift and low insertion loss variation with phase. Results of Reference (1) report an X-band microstrip circulator-coupled phase shifter with about 270° of phase shift and a total insertion loss modulation of 1.7 dB. Reference (2) reports X-band results with a 2.5 dB insertion loss with ±0.5 dB of insertion loss variation but only about 105° of phase shift.

The circuit approach used here is based on the well known reflection phase shifter, in which the through and coupled ports of a 90° hybrid are terminated in low-loss reactive networks. The other two ports of the hybrid form the circuit input and output. In this work we have used Lange couplers to realize the 90° hybrids and hyperabrupt varactor diode circuits for the terminating impedances.

The hyperabrupt active layer of the varactor can be controlled to achieve a capacitance versus voltage characteristic that offers the potential of large phase shifts with approximately linear phase versus voltage behavior.

The hyperabrupt varactor diodes are generally characterized by a capacitance versus voltage dependence of the form $C = C_{jo}/(1 + V/V_o)^{\gamma}$, where $\gamma > 1$. C_{jo} is the zero bias capacitance of the device and V_o is the built-in potential of the Schottky junction. The fact that $\gamma > 1$ in this equation indicates that the depletion layer capacitance decreases rapidly with applied reverse bias. This property is characteristic of hyperabrupt diodes, and sets them apart from the capacitance versus voltage properties of abrupt ($\gamma = 1/2$) or linearly graded ($\gamma = 1/3$) type doping profiles. This allows large tuning ratios, defined as C_{jo}/C_{jmin}, to be achieved.

Further insight into the relation between the varactor C(V) characteristic and the phase shifter circuit may be obtained by considering a simple capacitive termination with one node grounded and the other referenced to an impedance Z_o. If the capacitance in this example is realized by a varactor, then the phase angle of the reflection coefficient depends on reactance in the following way.

$$\phi(X_n) = 2 \arctan (X_n)$$

where X_n is the normalized reactance of the termination, given by,

$$X_n(V) = \frac{(1 + V/V_o)^{\gamma}}{\omega Z_o C_{jo}}$$

In many cases, phase linearity with voltage is a desirable feature. This functional dependence is determined by the above set of equations. The slope of the phase versus reactance curve decreases continuously as X_n increases because of the inverse tangent function. This variation must be compensated by the reactance vs voltage curve, which dictates that the slope of $X_n(V)$ must continuously increase with applied voltage. A necessary condition for this to occur is that the parameter γ must be greater than 1, so that hyperabrupt diodes are ideally suited for

CH2848-0/90/0000-0487$01.00 © 1990 IEEE

approximating linear phase. As can be seen from the equations, other parameters also play a role in determining the phase linearity. It may be shown that optimum values of ω, C_{jo}, and Z_o exist that will give the optimum linearity for a particular diode with $\gamma > 1$ (1).

VARACTOR DIODE CHARACTERIZATION

The varactor diodes used in the current phase shifter are commercially available silicon epitaxial mesa type devices. The measured 1-MHz capacitance vs voltage characteristic of a typical device is shown in Fig. 1. This graph covers the full capacitance swing of the device, corresponding to a voltage range of approximately 0 to -32 V. The device has a gamma value of about 1.1 for bias voltages of -4 V to -20 V. The gamma value decreases significantly for voltages outside of this range. This behavior is typical of hyperabrupt varactors in which the maximum gamma value is a constant generally in the range of 1 to 2 over a portion of the full voltage range. RF measurements were also performed on this diode by mounting the device as a termination at the end of a 50-Ω microstrip transmission line. The magnitude and angle of the reflection coefficient were measured as functions of both frequency and voltage. The capacitance values deduced from the phase vs voltage data were in close agreement with the values found from the 1-MHz C(V) measurement. Also, the variation in the magnitude of the reflection coefficient as a function of voltage indicated a device series resistance which decreased as bias became more negative. This is to be expected from the physical structure of the varactor since one component of the series resistance consists of the undepleted epitaxial material, which becomes thinner with more negative bias. For this commercial diode, the resistance value was near 4.5 Ω at 0-V bias and decreased to 2.5 Ω at 30-V bias.

CIRCUIT DESIGN

A basic schematic of the circuit is shown in Fig. 2, where the input and output ports are assumed to be matched to 50 Ω. The power incident at the input port is divided equally between the coupled and through ports of the hybrid and is reflected from the varactor networks. The reflected signal undergoes a phase change determined by the reflection coeffient of the terminating impedance. The power is then recombined at the isolated port of the hybrid which forms the circuit output. In the simplest case of an ideal diode termination, the reflection coefficient established by the diode follows the outer periphery of the Smith Chart through a specific phase range determined by the maximum capacitance variation of the varactor. The reflection coefficient also depends on the impedance level Z_o. The total phase range determines the amount of phase shift available from the circuit.

For real varactors with finite Q, the effective series resistance must be included in the circuit model. In this case, the reflection coefficient follows a constant resistance circle on the Smith Chart, and has a phase range determined by the capacitance variation of the diode. The effect of series resistance dominates the overall insertion loss of the phase shifter circuit and also determines the variation of insertion loss with applied voltage. A simple technique for compensating the bias dependence of insertion loss is to include a shunt resistor R_{comp} in parallel with the diode as shown in Fig. 3a (3). The value of this compensating resistor is related to Z_o and R_s by the relation,

$$R_{comp} = Z_o^2/R_s$$

The effect of this resistor is to transform the constant resistance locus to a circular locus that maintains nearly constant radius from the center of the Smith Chart. In this way, the phase shifter insertion loss becomes insensitive to changes in diode capacitance. The effect on the available phase shift range is negligible. The phase shift available from a single diode circuit may be doubled by using a dual varactor terminating impedance, as shown in Fig. 3b (3). This consists of two diodes and compensating resistors spaced at each end of a quarter wavelength transmission line of characteristic impedance Z_o. The reflection coefficient is referenced to an impedance $Z_o/2$ and is given by the equation,

$$\rho' = \frac{Z_T - Z_o/2}{Z_T + Z_o/2}$$

Z_T is the input impedance of the dual varactor circuit given by

$$Z_T = \frac{Z_L\,(Z_o^2/Z_L)}{Z_L + Z_o^2/Z_L}$$

in which Z_L is the input impedance of the single diode circuit. By eliminating Z_T from these equations, it is found that

$$\rho' = -\left[\frac{Z_L - Z_o}{Z_L + Z_o}\right]^2$$

Therefore, the overall reflection coefficient is determined by the squared reflection coefficient of the single varactor circuit. The doubling of the phase shift range by this relation is, of course, associated with twice the insertion loss as well. For a given varactor capacitance range, the available amount of phase shift may be increased by lowering the impedance level Z_o. This technique works well down to a certain impedance level after which the bandwidth of the circuit becomes impractically small. Therefore, the optimum design uses the highest impedance level that produces the necessary phase shift range. For the diodes used in the MIC circuit the optimum impedance level was found to be 60 Ω, so that the characteristic impedance of the 90° hybrid is 30 Ω.

The reflection phase shifter circuit constructed with this type of termination gives 180° of phase shift for a capacitance variation between 0.2 pF and 2 pF. To achieve the full 360° range, two identical 180° circuits are placed in cascade. The input and output ports include quarter-wave transformers to match between the 30-Ω level of the Lange couplers and the 50-Ω system level. The circuit is fabricated on a 10-mil-thick alumina substrate with bond wires to interconnect the fingers of each Lange coupler and to connect between the circuit and the varactor and resistor chip components. A photograph of the assembled circuit is shown in Fig. 4, where the cascaded 180° phase shift sections are apparent.

MEASURED PHASE SHIFTER RESULTS

The measured results over 9.5-10.5 GHz are summarized in Fig. 5 a,b,c,d. The relative phase shift plots in Fig. 5a use the zero bias state as the 0° reference for all other bias states. The phase shift range could be extended by using diodes with a lower C_{min} value. The insertion loss plot in Fig. 5b shows an average absolute value of about 5.3 dB, which includes approximately 0.5 dB of test fixture loss. The insertion loss modulation over this frequency band is within ±0.5 dB. The input and output return losses shown in Fig. 5c,d are similar because of the symmetrical design of the circuit.

The phase vs voltage characteristic at 10 GHz is shown in Fig. 6. The curve represents approximately linear behavior until C_{min} is approached at approximately -25-V bias. The effect of temperature on phase shifter performance is summarized in Fig. 7, where phase shift is displayed with temperature and bias voltage as parameters. Phase shift results are shown for the bias states 0 V, -15 V, -25 V and temperatures of -40°C, 20°C, and 60°C. As can be seen, the temperature change produces nearly the same incremental phase shift for all bias states, and therefore the relative phase shift from one bias state to the next is affected very little by changes in temperature.

The circuit described here is operated with the varactors in a reverse bias state, and, consequently, the DC power requirements are negligible. Only a single bias voltage is required for all eight varactors in the circuit so that very simple control circuitry may be used.

CONCLUSION

An X-band hybrid phase shifter circuit has been described which produces a large phase shift range with 4.8 dB of insertion loss and ±0.5 dB of insertion loss modulation over all phase states. The circuit design features that make this possible include referencing the reflection coefficient to an impedance below the standard 50 Ω, using the dual varactor terminations with compensating resistors as described previously, and forming a cascade of identical 180° phase shift sections.

ACKNOWLEDGEMENTS

The authors would like to thank P. Cline, R. Kroll, and M. Urcuyo for assistance in phase shifter circuit assembly and testing.

REFERENCES

(1) E. C. Niehenke, V. V. DiMarco, and A. Friedberg, "Linear Analog Hyperabrupt Varactor Diode Phase Shifters," 1985 IEEE MTT-S Digest, pp. 657-660.

(2) D. E. Dawson, A. L. Conti, S. H. Lee, G. F. Shade, and L. E. Dickens, "An Analog X-Band Phase Shifter," IEEE 1984 Microwave and Millimeter-Wave Monolithic Circuits Symposium, Digest of Papers, pp. 6-10.

(3) Robert V. Garver, "360° Varactor Linear Phase Modulator," IEEE Transactions on Microwave Theory and Techniques, Vol. MTT-17, No. 3, March 1969, pp. 137-147.

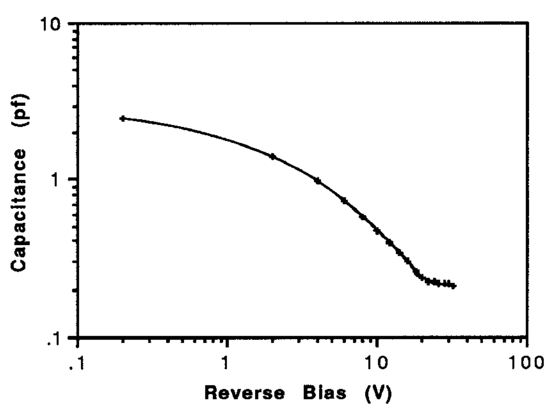

Fig. 1. Measured 1-MHz C(V) Characteristic of Commercial Varactor

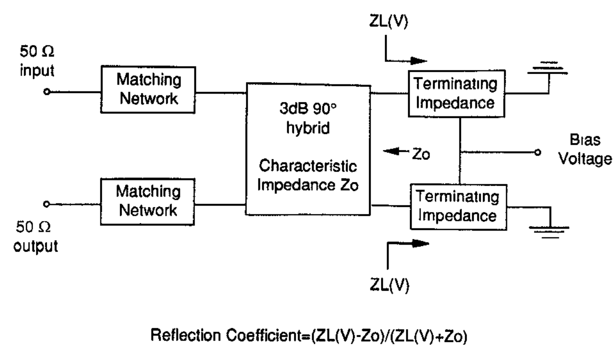

Fig. 2. Basic Schematic of Reflection Phase Shifter

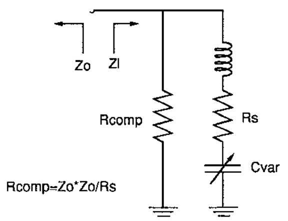

Fig. 3a. Single Varactor Termination With Compensating Resistor

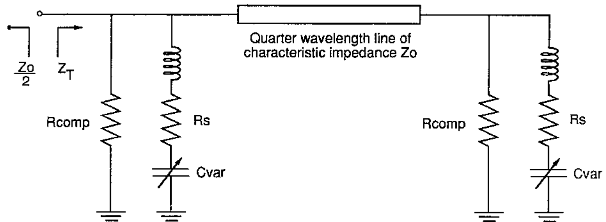

Fig. 3b. Dual Varactor Termination for Doubling Phase Shift Range

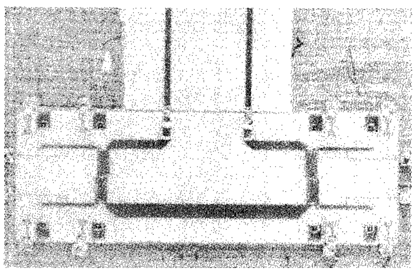

Fig. 4. Photograph of X-Band Phase Shifter Circuit

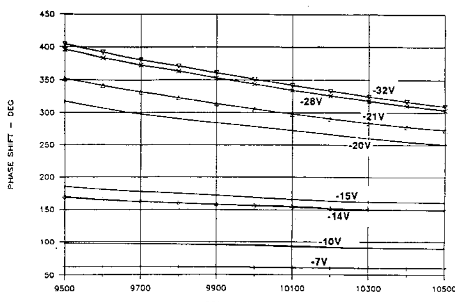

Fig. 5a. Relative Phase Shift (0-32 V)

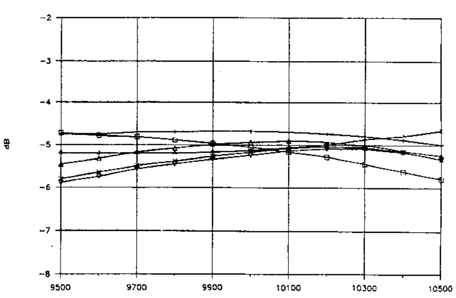

Fig. 5b. Insertion Loss (0-32 V)

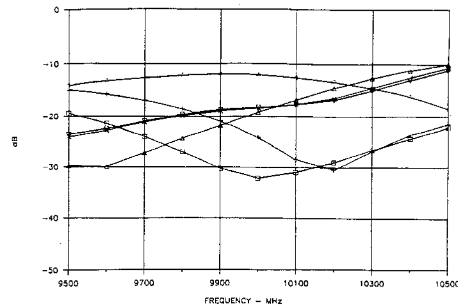

Fig. 5c. Input Return Loss (0-32 V)

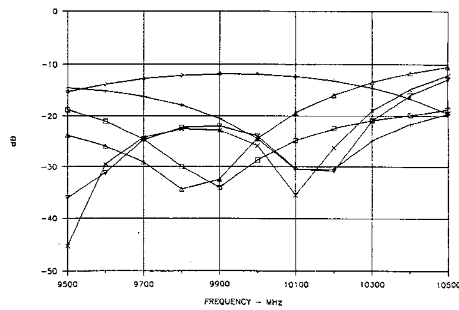

Fig. 5d. Output Return Loss (0-32 V)

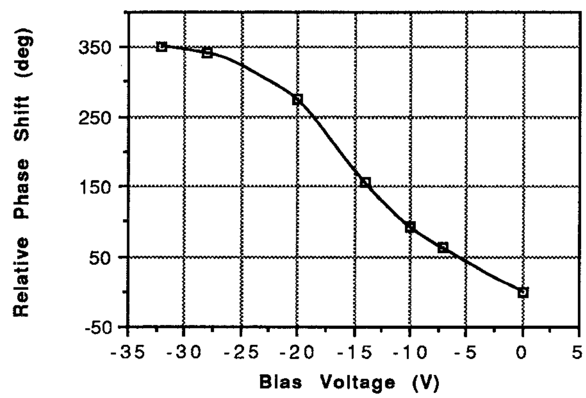

Fig. 6. Measured Phase vs Voltage Characteristic at 10 GHz

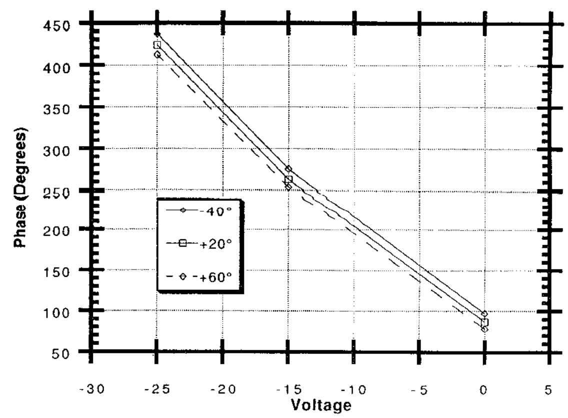

Fig. 7. Temperature Dependence of Phase Shift